JOURNAL OF RESEARCH of the National Bureau of Standards—C. Engineering and Instrumentation
Vol. 64C, No. 2, April–June 1960

Electrostatic Deflection Plates for Cathode-Ray Tubes. I. Design of Single-Bend Deflection Plates With Parallel Entrance Sections. II. Deflection Defocusing Distortion of Single-Bend Deflection Plates With Parallel Entrance Sections.

Lothar Frenkel [1]

(March 5, 1959)

In section I, a plate design system is offered which allows rapid and accurate determination of mechanical plate parameters to achieve given electrical plate characteristics. The design is suitable for single-bend plates with parallel entrance sections. The design curves were calculated under the conventional assumptions of small deflection theory, but corrections for the entrance and exit fields are included. The method of calculating the curves and corrections is indicated in an appendix.

Section II deals with deflection defocusing of such plates, a convenient formula for calculating the defocusing distortions of single-bend deflection plates is derived and compared with experiment. This type of distortion is proportional to the square of the deflection angle and is shown to be sensitive to plate design. In general, long deflection plates give lower distortions while the most "economical" plates yield larger distortions. Post deflection is shown to lead to increased distortions.

I. Design of Single-Bend Deflection Plates With Parallel Entrance Sections

1. Introduction

Designing a cathode-ray tube is as much an art as a science; experience and the correct choice of compromises between various parameters are both important. Experience suggests that the best tubes are designed in close cooperation between instrument designers and tube engineers. In many instances the tube designer in these discussions has nothing to go by except his experience, and any information of a quantitative nature is welcome. Such information is provided for the gun performance, for instance, by the work of H. Moss [1],[2] and it is hoped that the design system offered here will contribute to establishing this kind of information for the design of plates.

The design of cathode-ray tube deflection plates of specific characteristics is complicated by the choice of parameters available. Thus the shape of the plate may range from parallel plates to continuously flared plates, and the initial spacings from 0.030 in. to 0.1 in.

Given a definite plate shape, one can solve the equation of motion and thus determine the sensitivity and scan. The converse is not true, however, and tube designers have long needed a method which enables them to decide on suitable compromises without having to check design possibilities by laborious experiment. The design method offered here has been checked in many experiments over a span of five years and has been found accurate within the limits imposed by mechanical tube assembly.

2. Qualitative Considerations

A successful cathode-ray tube is one which will allow the ultimate utilization of the characteristics of the vertical amplifier for which it was designed. Such amplifiers are generally limited in voltage swing and bandwidth by the capacitance of the load which they have to drive. The requirements on the cathode-ray tube are therefore to provide best deflection sensitivity consistent with the required scan, capacitance, and writing speed. The most sensitive plates would be flared in such a manner that the fully deflected beam smoothly follows the positive deflection plate. Such optimum plate shapes have been described in the literature [2].

In practice continuous curvature is difficult to obtain, and approximation by bending is preferred. For the present design, single-bend plates with parallel entrance sections have been chosen. Such plates approach the optimum very closely, particularly in scan-limited tubes, which are used in the most advanced applications.

3. Theory

The most important design characteristics of a plate pair are its inverse sensitivity (say, in volts per inch) and the scan (in inches). The product of these parameters determines the maximum potential difference applied to the plates.

[1] Formerly, Tektronics—Portland, Oregon. This work was done at the A. B. DuMont Laboratories in 1953 and 1954.
[2] Figures in brackets indicate the literature references at the end of section I.

When, as is usually the case, the plates are arranged symmetrically about the undeflected beam, then one-half of this potential, V_{max}, determines the dimensions of the plate. Consider the parallel section first, as in figure 1. We arbitrarily stipulate that the width of the beam, w, should be $2/3\ s$, where s is the spacing of the plates, and that ¼ of the beam should be cut off by the plate edge. The deflection at the exit end is then given by:

$$y_1 = s/3 = e/m \int_0^{t_a}\int_0^{t_x} (V_{max}/s)\,dt\,dt \qquad (1)$$

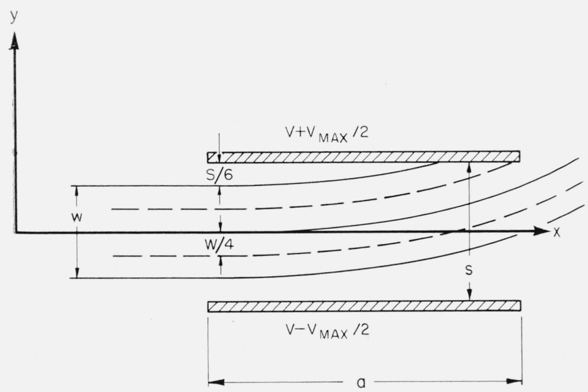

FIGURE 1. *The parallel section.*

where a is the length of plate. This equation serves to establish a as a function of s and V_{max}.

During transit in the flared section the beam is further deflected. The deflection due to the flared section alone gives, with reference to figure 2,

$$y_2 = e/m \int_c^{t_b}\int_c^{t_r} (V_{max}/\alpha r)\,dt\,dt, \qquad (2)$$

where we have assumed cylindrical field symmetry. The total deflection y_3 at the exit end of the combined plate is due to the deflection in each section plus the displacement in the flared section due to acceleration in the first, i.e.

$$y_3 = e/m \int_0^{t_a}\int_0^{t_x} (V_{max}/s)\,dt\,dt$$

$$+ e/m\left[\int_0^{a} (V_{max}/s)\,dt\right] t_{cb}$$

$$+ e/m \int_c^{t_b}\int_c^{t_r} (V_{max}/\alpha r)\,dt\,dt, \qquad (3)$$

where t_{cb} is the transit time from c to b. We now stipulate arbitrarily that at the exit end of the combined plate one-half of the beam should be cut off, i.e.,

$$y_3 = \alpha b/2. \qquad (4)$$

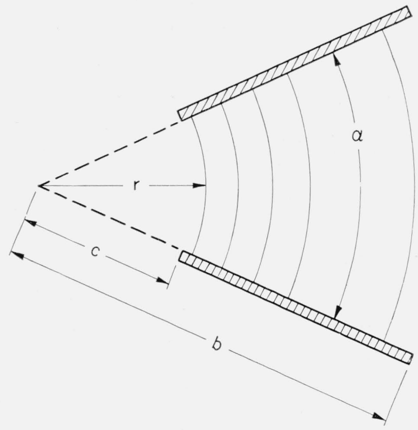

FIGURE 2. *The flared section.*

Thus, eqs (3) and (4) serve to give α as a function of s, a, V_{max}, and any arbitrary length of plate ($L = a + b - c$). In practice, α must be determined graphically. The sensitivity or inverse sensitivity may now be calculated for known screen distances. Additional assumptions, corrections, and the general formula are given in appendix 1 and 2. It should be noted that the determination of plate shape involves the simultaneous solution of eqs 1 to 4 and eq (a1) of appendix 3, after arbitrary decisions on spacing or length have been made.

On the other hand, the designs presented here are based on a large number of theoretical calculations in which the sensitivity was calculated as above after spacings, total lengths, and maximum voltages were arbitrarily chosen. As a result of calculating a large number of designs and tabulating the results, sets of curves are obtained which permit the selection of a plate shape for a given sensitivity and scan.

4. Method of Design

There are 3 sets of curves concerned with plate design parameters. All are based on the characteristic peak to peak plate cutoff voltage of 2 V_{max}. This may be defined as follows: Given a standard accelerating potential of 1 kv, $2V_{max}$ is the product of the desired total scan, times the inverse sensitivity (in volts per unit deflection).

The first set of curves A1 to A7 gives the inverse sensitivity as a function of $2V_{max}$. There are several sheets of curves each for a given total length of plate L. On each sheet there are several curves each for a specific entrance spacing s. The first set of curves thus serves to determine immediately what length and spacing are necessary to achieve a given scan and sensititivity.

The remaining two sets of curves B and C1 to C7 serve to establish the design completely by giving the length of the straight section and the angle of bend as functions of the parameter $2V_{max}$ and the length and spacing chosen from the first set. Thus it is not necessary to consult these sets for the initial discussion of a new cathode-ray tube design.

5. Post Acceleration

Post acceleration does not affect the value of $V_{\max}$ for a given plate but increases the inverse sensitivity by an amount variously called intensifier factor or compression factor. The factors vary depending on the bulb shape and the shape and the degree of continuity of the post accelerator. It differs also for the front and back plates of the same tube. To facilitate the design of post deflection accelerator tubes a set of curves D giving compression ratios for various tube types as a function of accelerator potential to anode potential ratio is included.

The compression factors for types quoted will apply approximately to all tubes of similar design. Type I has a straight-sided (T-shaped) bulb with 3 accelerator bands; type II has 1 accelerator band on a conical bulb; and type III uses a continuous accelerator in a bulb of exponential shape. For exact information the factors must be established experimentally for any given bulb shape, accelerator bands, and tube geometry. In general the continuous accelerator spiral gives the lowest loss in sensitivity.

6. Correction for Tube Length

The values of inverse sensitivity must be corrected by the ratio of the effective distance to the screen to the effective distance applicable for each sheet. This may be done as follows: The effective distance, with sufficient accuracy, may be taken as the distance of the screen from the exit end of the plate plus half the plate length. The distance D quoted on each sheet is the distance of the exit end of the plates on that sheet from the screen of the tube. The corresponding assumed effective distances therefore are greater in each case by about one-half of the plate length applicable to that sheet. The reason for this arrangement is that the design is needed mostly for the vertical plates of sensitive instrument tubes, and in considering the effect of changing plate lengths it is convenient to fit all designs to a standard length of tube.

7. Beam Width

The plate designs are based on an assumed beam width of ⅔ of the spacing s of the parallel section of the plates. If the limiting aperature size is taken in this manner cutoff is sharp and clean. For the highest performance types of tubes one might sacrifice edge performance, and values of ⅘ s for the diameter of the limiting aperture have been used in some tubes with consequent gain in brightness and definition in the center area of the screen.

Appendix I. Summary of Steps in Designing a Plate

1. *Establish the desired characteristics.* (a) Anode potential; (b) Post deflection accelerator ratio; (c) Desired inverse sensitivity; (d) Desired scan; and (e) Tube length.

2. *Find 2* V_{max}. Multiply the inverse sensitivity above by the desired scan.

3. *Normalize inverse sensitivity and 2* V_{max}. This is done by dividing both quantities by the anode potential in kilovolts.

4. *Adjust normalized inverse sensitivity for post deflection.* This is done by finding the compression factor from curves D and reducing the inverse sensitivity by it.

5. *Adjust normalized inverse sensitivity for tube length.* It is now necessary to select an approximate value of plate length and to find the corresponding value of D from the curves. The value for inverse sensitivity is then adjusted as outlined previously.

Steps 1 to 5 are easily accomplished, and the information is now available for a complete design.

6. *Establish a spacing* s *and complete design.* By consulting the set of curves A, a spacing may be selected for each of various possible plate lengths. This involves a compromise in terms of beam size, etc. When this choice has been made the straight length and bend angle may be found directly from the remaining two sets of curves. If it is found that the design chosen leads to unrealistic spacings or length it is necessary to modify the electrical characteristics and to try again. Since the whole procedure takes only a short time, a suitable compromise can be found quickly.

Appendix II. Corrections

An accurate small signal theory is given by Hutter [3]. More specific formulas [2, 4] have appeared in the literature from time to time, and the present method of design is based on the conventional assumptions of constant transit velocity and cylindrical field geometry in the flared part. Three corrections are, however, included in the final calculation which should be stated here.

(1) It is assumed that the field of the parallel section extends a distance $s/2$ beyond the plates.

(2) The electron with maximum deflection is assumed to travel along an equipotential line close to the positive deflection plate. Accordingly the field is inclined to the vertical by about the angle which the plate subtends with the axis. This means that the transverse acceleration results in a reduction of axial velocity. The term describing the transverse acceleration is corrected by the cosine of the plate angle, and the axial velocity through the drift space is corrected accordingly.

(3) It is also assumed that the axial motion is further retarded at the exit end while the transverse motion remains unchanged. Thus an electron just passing the edge of the positive plate has energy $e(V+V_{\max}/2)$, but a short distance farther its energy is again eV and remains so to the screen. The corresponding field is axially directed since it usually terminates on grounded structures just ahead of the plates.

The axial velocity is reduced according'y.

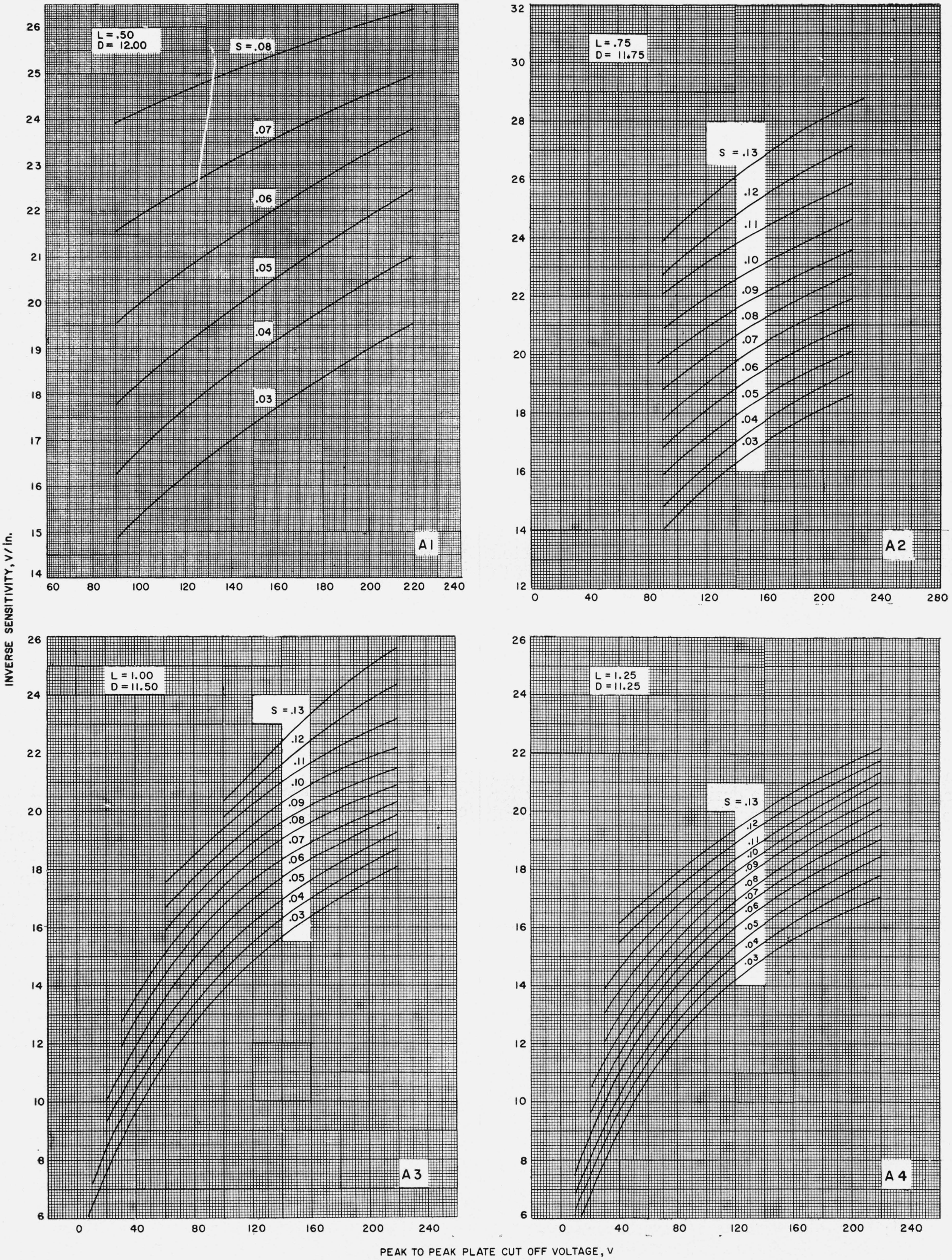
INVERSE SENSITIVITY, V/In.
PEAK TO PEAK PLATE CUT OFF VOLTAGE, V
L = .50
D = 12.00
S = .08
.07
.06
.05
.04
.03
A1
L = .75
D = 11.75
S = .13
.12
.11
.10
.09
.08
.07
.06
.05
.04
.03
A2
L = 1.00
D = 11.50
S = .13
.12
.11
.10
.09
.08
.07
.06
.05
.04
.03
A3
L = 1.25
D = 11.25
S = .13
.12
.11
.10
.09
.08
.07
.06
.05
.04
.03
A4

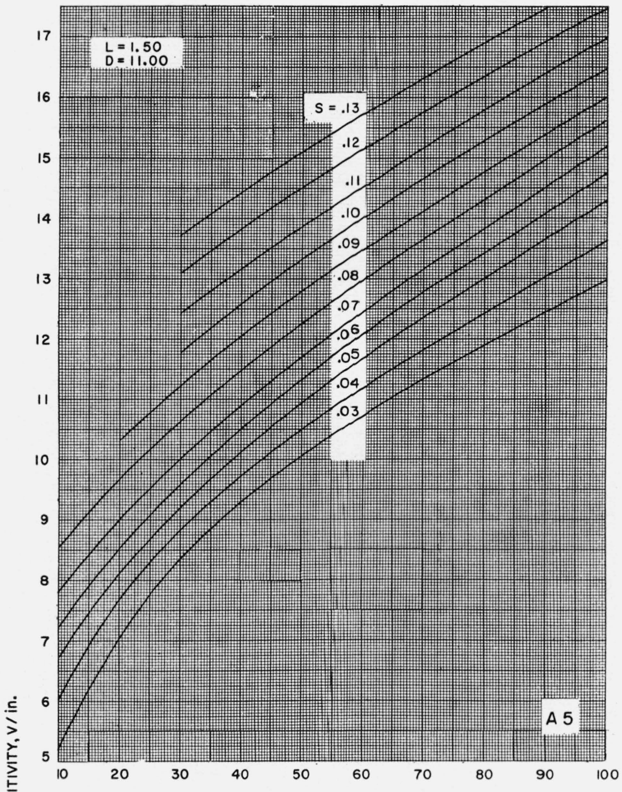
L = 1.50
D = 11.00
S = .13
.12
.11
.10
.09
.08
.07
.06
.05
.04
.03
A 5
INVERSE SENSITIVITY, V/ in.
5 6 7 8 9 10 11 12 13 14 15 16 17
10 20 30 40 50 60 70 80 90 100

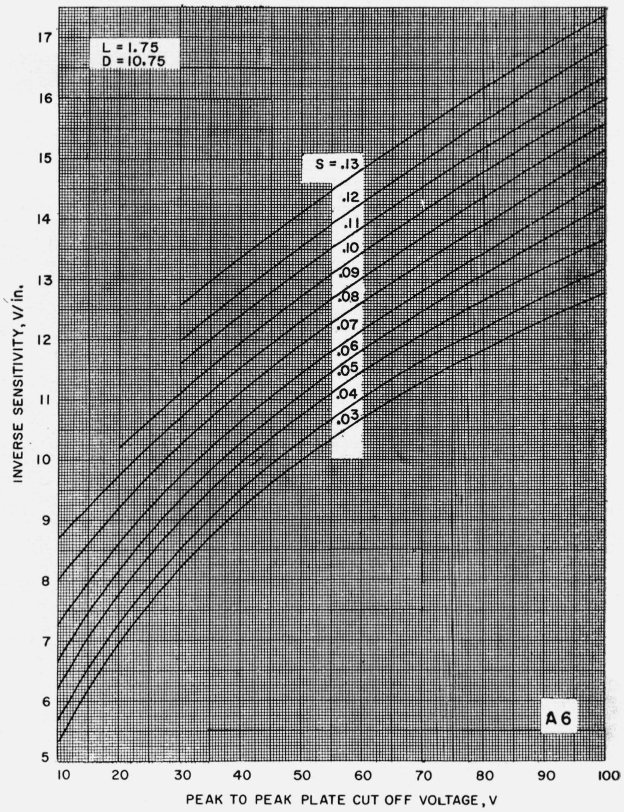
L = 1.75
D = 10.75
S = .13
.12
.11
.10
.09
.08
.07
.06
.05
.04
.03
A 6
INVERSE SENSITIVITY, V/ in.
5 6 7 8 9 10 11 12 13 14 15 16 17
10 20 30 40 50 60 70 80 90 100
PEAK TO PEAK PLATE CUT OFF VOLTAGE, V

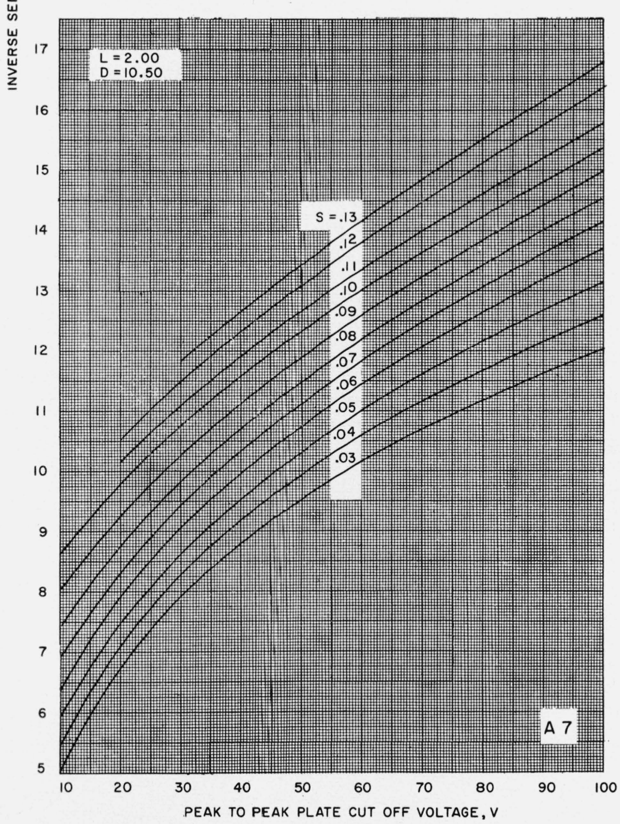
L = 2.00
D = 10.50
S = .13
.12
.11
.10
.09
.08
.07
.06
.05
.04
.03
A 7
5 6 7 8 9 10 11 12 13 14 15 16 17
10 20 30 40 50 60 70 80 90 100
PEAK TO PEAK PLATE CUT OFF VOLTAGE, V

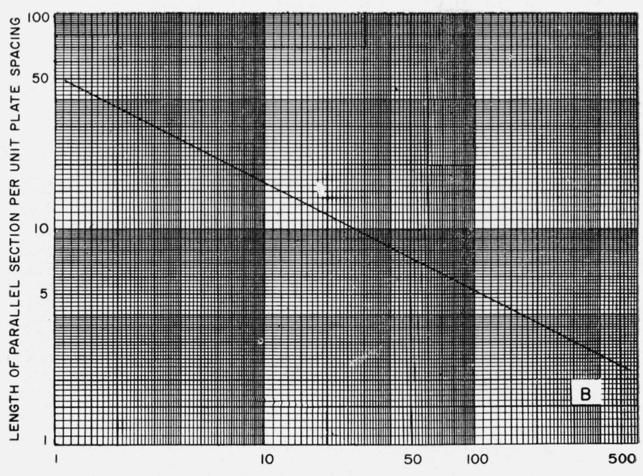
LENGTH OF PARALLEL SECTION PER UNIT PLATE SPACING
1 5 10 50 100
1 10 50 100 500
B
PEAK TO PEAK PLATE CUT OFF VOLTAGE, V

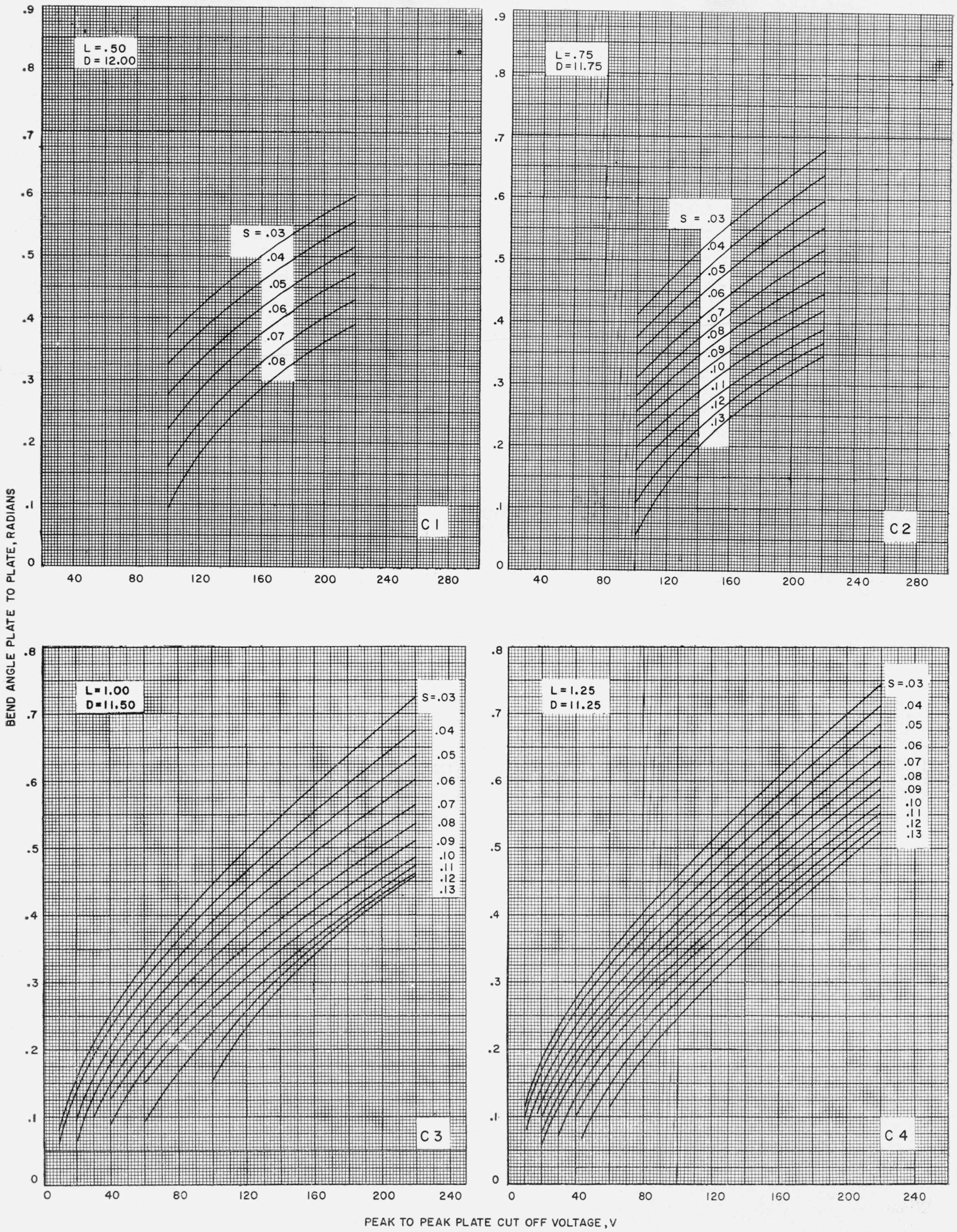
L = .50
D = 12.00
S = .03
.04
.05
.06
.07
.08
C 1
L = .75
D = 11.75
S = .03
.04
.05
.06
.07
.08
.09
.10
.11
.12
.13
C 2
L = 1.00
D = 11.50
S = .03
.04
.05
.06
.07
.08
.09
.10
.11
.12
.13
C 3
L = 1.25
D = 11.25
S = .03
.04
.05
.06
.07
.08
.09
.10
.11
.12
.13
C 4
BEND ANGLE PLATE TO PLATE, RADIANS
PEAK TO PEAK PLATE CUT OFF VOLTAGE, V

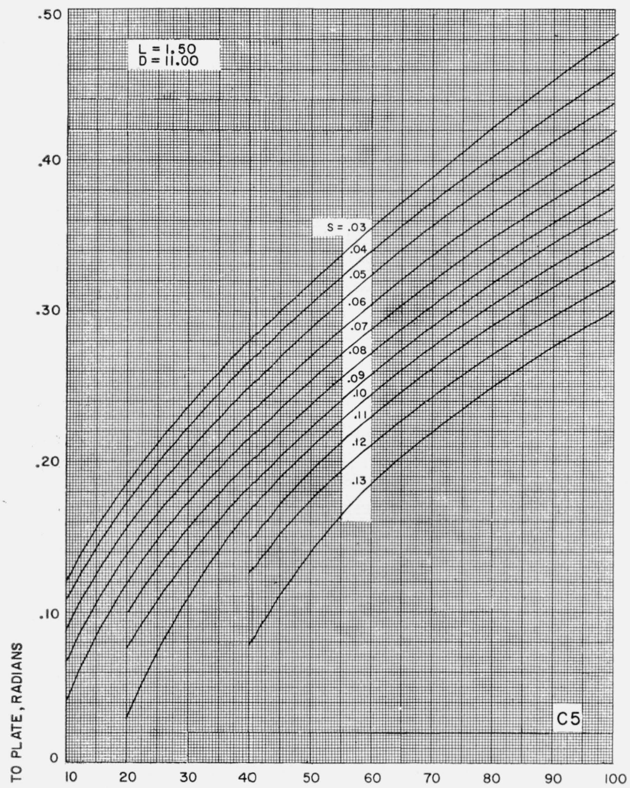
L = 1.50
D = 11.00
S = .03
.04
.05
.06
.07
.08
.09
.10
.11
.12
.13
C5
BEND ANGLE PLATE TO PLATE, RADIANS

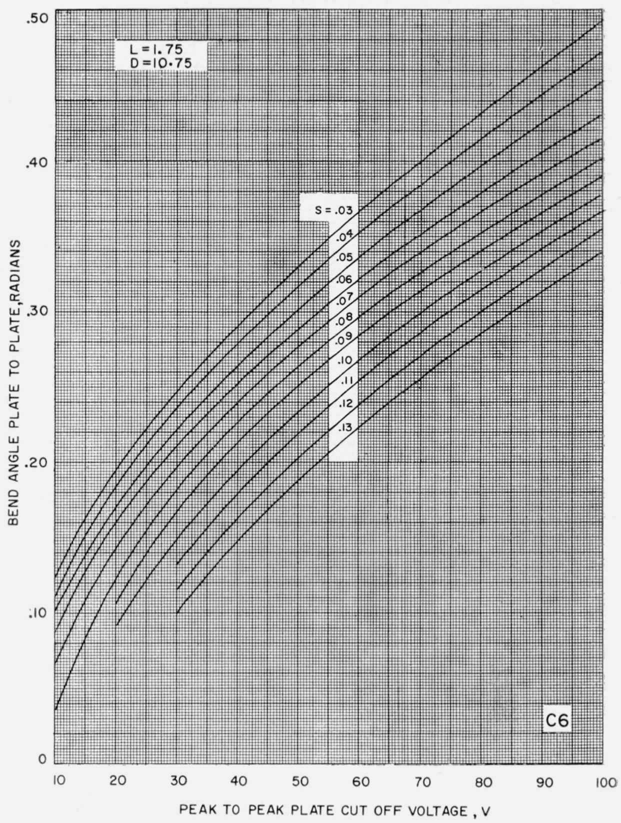
L = 1.75
D = 10.75
S = .03
.04
.05
.06
.07
.08
.09
.10
.11
.12
.13
C6
BEND ANGLE PLATE TO PLATE, RADIANS
PEAK TO PEAK PLATE CUT OFF VOLTAGE, V

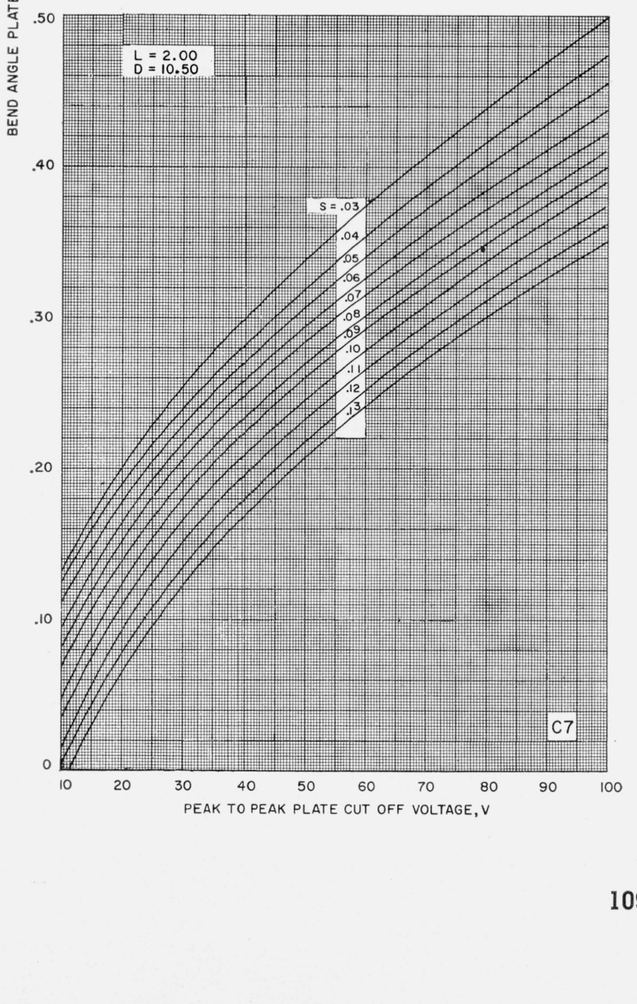
L = 2.00
D = 10.50
S = .03
.04
.05
.06
.07
.08
.09
.10
.11
.12
.13
C7
PEAK TO PEAK PLATE CUT OFF VOLTAGE, V

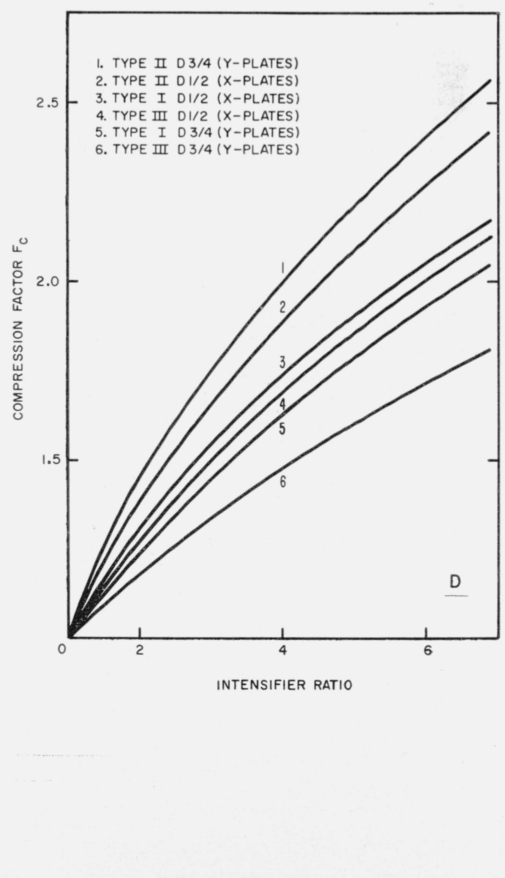
1. TYPE II D 3/4 (Y-PLATES)
2. TYPE II D 1/2 (X-PLATES)
3. TYPE I D 1/2 (X-PLATES)
4. TYPE III D 1/2 (X-PLATES)
5. TYPE I D 3/4 (Y-PLATES)
6. TYPE III D 3/4 (Y-PLATES)
COMPRESSION FACTOR F_C
INTENSIFIER RATIO
D

Appendix III. Theory

The general formula used for the design was:

$$y=\left(\frac{U}{VF_c}\right)\left[1+\frac{U}{4V}\left(1+\log\frac{b}{c}\right)\right]\left\{\frac{\overline{a}^2}{4s}+\frac{\overline{a}(b-c)}{2s}\right.$$

$$\left.+D\left[\frac{a}{2s}+\frac{1}{2\alpha}\left(1-\frac{\alpha^2}{4}\right)\log\frac{b}{c}\right]+\frac{1}{2\alpha}\left[c-b\left(1-\log\frac{b}{c}\right)\right]\right\} \tag{a1}$$

where

- $\overline{a}$ is the length of the straight section plus ½ of the spacing, s,
- b is the terminal length of the flared section in polar coordinates,
- c is the initial point of the flared section in polar coordinates,
- D is the distance to the screen of the exit end of the plates,
- $+V$ is the anode potential,
- $V+U/2$, $V-U/2$ are the plate potentials,
- y is the deflection at the screen,
- F_c is the compression ratio,
- s is the spacing of the plates, and
- α is the plate angle.

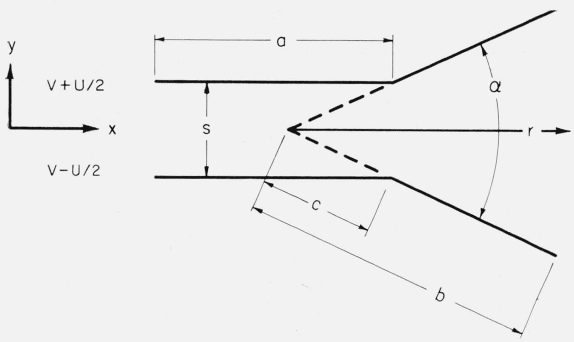

FIGURE 3. *Flared plate with parallel entrance.*

Formula 1 was derived by integrating and summing the equations of motion of the electron in the corresponding regions of the plate and the drift space.

In the parallel section, for example, we have for transverse velocity v_y and position y,

$$v_y=(eU/ms)\int_0^{t_x} dt, \tag{a2}$$

$$y=(eU/ms)\int_0^{t_{\overline{a}}}\int_0^{t_x} dt\, dt. \tag{a3}$$

For the flared region these quantities are

$$v_y=(eU/m\alpha)\int_{t_c}^{t_r}(1/r)dt, \tag{a4}$$

$$y=(eU/m\alpha)\int_{t_r}^{t_b}\int_{t_c}^{t_r}(1/r)dt\, dt. \tag{a5}$$

We also have, according to our assumption, the energy equation determining the axial velocity.

$$mv_x^2=2eV, \tag{a6}$$

and therefore,

$$dt=dx/\sqrt{2eV/m}, \tag{a7}$$

applying eq (a2) to (a5) to the corresponding regions, integrating by means of (a7) and applying the corrections outlined before there results eq (a1).

8. References

[1] H. Moss, The electron gun of the cathode ray tube, J. Brit. Inst. Radio Engrs. **6,** 99, (1946).

[2] I. G. Maloff and D. N. Eppstein, Electron optics in television, p. 100 (McGraw-Hill Book Co., Inc., New York, N. Y., 1938).

[3] R. G. E. Hutter, Electron beam deflection, J. Appl. Phys. **18,** 740, (1947).

[4] R. Benham, Inclined deflection plates, Wireless Eng. **13,** No. 148, p. **10** (1936).

II. Deflection Defocusing Distortion of Single-Bend Deflection Plates With Parallel Entrance Sections

1. Introduction

Cathode-ray oscilloscope displays generally suffer from a broadening of the trace with increasing deflection [1].[1] This is known as deflection distortion and has been treated in the literature in a general way [1, 2, 3].

Many standard cathode-ray tubes use single-bend plates with parallel entrance sections since these plates are both convenient and sensitive. A graphical design method for such plates has been described in section I. We now deal primarily with the calculation of the deflection distortion due to plates of this type.

2. Distortions Due to the Parallel Entrance Section

Let V be the mean potential in the plate region with respect to the cathode,
- U be the deflection potential across the plates,
- a be the length of the straight section,
- s be the plate spacing,
- e be the charge of the electron,
- m be the mass of the electron,
- F_1, F_x, F_y be field components,
- v_1, v_x, v_y be velocity components,
- E be a symbol for energy, and
- w be the width of the beam.

Since electron energy at any point is given by the potential of the point in the field, we see that electrons entering the plate at A and B (fig. 1) respectively

[1] Figures in brackets indicate the literature references at the end of Section II.

have energies differing by

$$\Delta E = eUw/s. \tag{1}$$

Further, we see from figure 1 that this difference is nearly all due to the difference in horizontal velocity, since the vertical field components acting on the electrons entering the field are equal while the horizontal components are opposite.

We have during transit:

$$\text{field} = Fy = U/s \tag{2}$$

$$\text{force} = eU/s \tag{3}$$

$$\text{accel} = eU/ms \tag{4}$$

$$\text{time} = a/v_x \tag{5}$$

therefore,

$$vy = eaU/mSV_x, \tag{6}$$

whence the exit angle for small deflections is given by:

$$\theta \approx \tan\theta = eUa/msv_x^2 \tag{7}$$

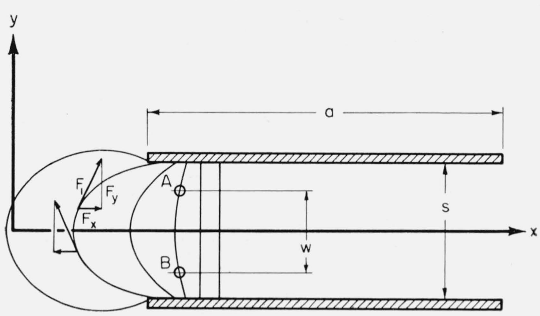

FIGURE 1. *The fringe field in the parallel section.*

But v_x differs for the two electrons, and to find the distortion we differentiate θ with respect to the entrance ordinate y.

We note that generally

$$E = mv^2/2 \tag{8}$$

and

$$E = e(V + yU/s) \tag{9}$$

or, combining (8) and (9)

$$v^2 = 2e(V + yU/s)/m \tag{10}$$

and since, as we have seen, for purposes of energy computations v equals v_x, we get for θ

$$\theta = aU/2s(V + yU/s) \tag{11}$$

and by differentiation

$$\frac{d\theta}{dy} = -\frac{aU^2}{2s^2(V+U/s)^2}. \tag{12}$$

Using w for the separation dy of the two extreme electrons and substituting eq (11) in (12) we find:

$$\Delta\theta = -2w\theta^2/a. \tag{13}$$

Thus the distortion varies as the square of the deflection angle and linearly with beam width. We also note that it varies inversely as the plate length.

3. Flared Section

We will assume that the field in the flared section is cylindrically symmetrical.

One further assumption will be made which requires some discussion. We will again assume that the entire energy difference for the extreme electrons is due to the difference in v_x. This assumption may be justified as follows. The mean energy difference of the electrons at extreme ends of the cross section is of the order of U divided by the ratio of plate spacing at some arbitrary point to beam width. Since the deflecting field decreases as the spacing increases we may assume the effective ratio to be about 2 or 3 for plates in which the initial spacing is comparable to the beam width. For such plates the Y-directed velocity after transit through the plates corresponds to a kinetic energy of the order of U. Thus it follows that the energy differences across the beam are substantial fractions of the deflection energy. But it may be observed experimentally that the distortion is only a small fraction of the total deflection. Thus the energy differential involved in the vertical motion of the electrons in the cross section is negligible.

Let us express this analytically:

In figure 2, let

c = the radius at the entrance,
b = the radius at the exit,
α = the angle of flare, and
g = the final opening.

Then

$$mv_x^2/2 = e\alpha(V + yU/\alpha x - \epsilon). \tag{14}$$

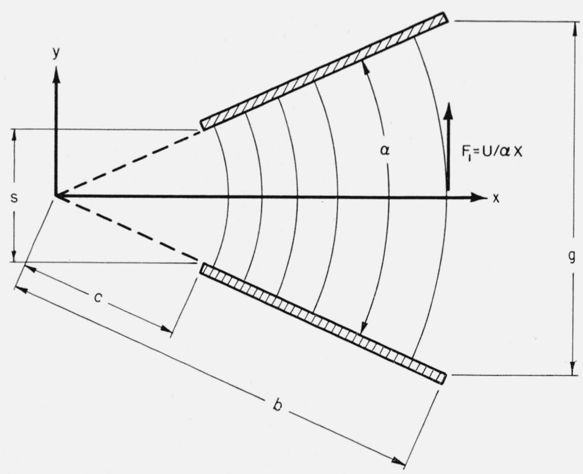

FIGURE 2. *The flared section.*

Here is a correction for the fact that some energy is contained in the vertical motion of the electron. Our assumption now states that ϵ may be larger than $yU/\alpha x$, but the differential of ϵ with respect to y is negligible compared to the differential of $(yU/\alpha x)$, at least in those parts of the field where deflection is effective. With these assumptions we proceed as before:

$$F_y = (U)/\alpha x) \text{ approx} \tag{15}$$

$$(\text{acceleration})\ y = eU/m\alpha x. \tag{16}$$

But since the acceleration now depends on x we have to integrate to find v_y:

$$v_y = eU/m\alpha \int_{t_c}^{t_b} (1/x)\, dt \tag{17}$$

and since $dt = dx/v_x$ (18)

$$v_y = eU/m\alpha \int_c^b 1/(v_x x) dx. \tag{19}$$

For small angles we may sum the increment:

$$\theta = (eU/m\alpha) \int_c^b 1/(v_x^2 x) dx. \tag{20}$$

Substituting for v_x^2 from (14) we have

$$\theta = \frac{U}{2\alpha} \int_c^b \frac{dx}{x(V + yU/\alpha x - \epsilon)}. \tag{21}$$

To find the defocusing effect we differentiate (21) with respect to y, remembering that $d\epsilon/dy = 0$; hence,

$$\frac{\partial\theta}{\partial y} = \frac{U}{2\alpha} \int_c^b \frac{U dx}{(V + yU/\alpha x - \epsilon)^2 \alpha x^2}. \tag{22}$$

We may now integrate (21) and (22), disregarding small quantities, to get

$$\theta = (U/2\alpha V) \log (b/c), \tag{23}$$

and

$$\Delta\theta = -dy \frac{U^2}{2\alpha^2 V^2} \left(\frac{b-c}{bc} \right). \tag{24}$$

Thus, $d\theta$ depends on U^2, and θ on U; hence in the inclined section $d\theta$ again depends on θ^2 and on $w = dy$, but its dependence on plate shape is now complicated as it involves log (b/c).

4. Total Distortion

A formula may now be established which allows direct investigation of the distortion of various plates designs. Let D be the distance to the screen; then the total broadening of the line will be

$$\Delta y = D(d\theta_1 + d\theta_2) \tag{25}$$

where $d\theta_1$, $d\theta_2$ are the distortions of the straight and flared sections, respectively. Substituting in (25) from (12) and (24) we get, after some rearranging:

$$\Delta y = -\frac{wDU^2 a}{2s^2 V^2} \left[1 + s \frac{(g-s)}{\alpha g a} \right]. \tag{26}$$

Here c and b have been eliminated by

$$\alpha c = s, \tag{27}$$

and

$$\alpha b = g, \tag{27a}$$

respectively. For practical designs (26) may be further simplified since g is much larger than s, i.e.,

$$\Delta y = -\frac{wDU^2 a}{2V^2 s} \left(1 + \frac{s}{\alpha a} \right). \tag{28}$$

Equation (28) is useful in comparing the distortions of various possible designs. Thus, when using the plate designs described in section I of this paper, the parameters in eq (28) may be found from the electrical characteristics required of the plate, and it is possible to take distortions into consideration when discussing a particular design. An example of the application of formula 28 to three experimental plates for a tube is given in table 1. Plate C is about twice

TABLE 1

A	B	C
$W=$ 030 in.	$W=$ 030 in.	$W=$030 in.
$D=$ 10.50 in.	$D=$ 12.25 in.	$D=$ 11.25 in.
$U=$ 150 v (full scan)	$U=$ 125 v (full scan)	$U=$ 85 v (full scan)
$a=$ .220 in.	$a=$ .210 in.	$a=$ .300 in.
$s=$ .060 in.	$s=$ .050 in.	$s=$ .060 in.
$V=$1675 v	$V=$1675 v	$V=$1675 v
$\alpha=$ .600 rad	$\alpha=$ .535 rad	$\alpha=$ .500 rad
$\frac{s}{\alpha a}=$ .450	$\frac{s}{\alpha a}=$ .445	$\frac{s}{\alpha a}=$ .400
$\Delta y=$ .128	$\Delta y=$ .124 in.	$\Delta y=$ .036 in.

as long as the other plates and may be seen to have only about one-fourth as much distortion. For a given plate length, increased sensitivity gives slightly better distortion characteristics, but generally distortions are determined by the desired characteristics of the plate.

5. Post Accelerator Field

Post acceleration generally reduces a scan pattern by the so-called compression factor shown in figure D of the plate design curves (see 5, section I). Since distortions are essentially a scan pattern they, too, are reduced by post acceleration, and eq (28) must be modified accordingly:

$$\Delta y = -\frac{wDU^2 a}{2F_c s^2 V^2} \left(1 + \frac{s}{\alpha a} \right). \tag{29}$$

In evaluating the distortions of monoaccelerators versus post accelerators it must be remembered that the deflection voltage requirements in the latter increase by the factor F_c. In eq (29) therefore, at equal deflection, Δy would be increased by a factor of F_c since for a given plate and for a fixed deflection, U would have to be increased as post acceleration is applied.

6. Agreement With Experiment

Maloff and Eppstein [1] have stated that distortions due to deflection in well-designed tubes are several times less severe than those to be expected from elementary theory. It is interesting therefore to see how eqs (28) or (29) compare with experiment. A typical experiment is shown in figure 3. The

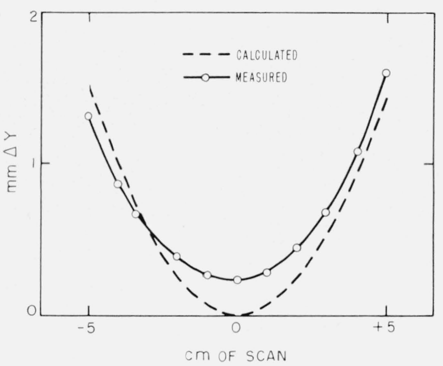

FIGURE 3. *Deflection defocusing.*

plate here is similar to plate A of table 1 but a compression factor of $F_c = 2$ applies. The agreement between calculated and experimental values are seen to be good in this instance. When making observations of deflection defocusing some points have to be carefully considered. Most modern plates are marginal, i.e., they intercept some of the beam toward the edge of the scan, and therefore the spot there tends to be less distorted than it would be theoretically. Another point of experimental significance is the mode of focusing. Consider for instance figure 4 in which 2 positions are shown for the screen.

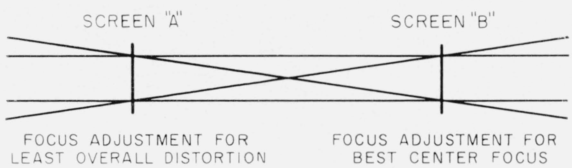

FIGURE 4. *Two possible focus adjustments relative to screen position.*

Position *a* shows an "underfocused" beam while position *b* corresponds to an overfocused beam. It is clear that deflection distortion, which consists of a focusing action with deflection, will be more effective in position *b* than in position *a*. The conclusion is that defocusing depends on the adjustment of the focusing lens and on the nature of beam formation about which not much is known.

7. Corrections for Defocusing

Qualitative reasoning suggests that no effective correction can be found which does not simultaneously result in severe deflection linearity distortion. This may be seen as follows: Since Δy is a negative function of y, deflection results in overfocusing. Nothing can be done about this in a nearly parallel section which is present in any deflection plate, for in such a region the assumptions made here are rigidly true.

At the exit end of the plates however, where the beam is already deflected across the axis, our assumptions do not hold, and the field may be shaped in such a manner as to deflect the electron traveling closer to the positive plate more than the electron at the other end of the cross section. If this is done it is clear that the correction is applied in a region of rapidly increasing separation of the entire beam from the axis. Thus what is required here is a variation of the effective strength of the deflection field in a transverse direction which is effective over the cross section of the beam. Consider now the effect of such a field on the central electron in a beam. As the deflection is increased the central electron travels in regions of increasingly effective deflection fields, and consequently the overall deflection becomes nonlinear.

The foregoing conclusion is particularly true of arrangements employing corrective static lenses such as positive wires lined up parallel to the exit edge of the plates.

In contrast with the qualitative argument given above, detailed mathematical treatment has led other authors [3, 4, 5], to propose plate shapes for which various degrees of correction are claimed.

8. Conclusions

Deflection defocusing in single-bend plates with parallel entrance sections is approximately proportional to the square of the deflection, it is linearly dependent on beam width, and is roughly inversely proportional to plate length and is therefore susceptible to changes in plate design.

9. References

[1] I. G. Maloff and D. W. Eppstein, Electron optics in television, p. 203 (McGraw-Hill Book Co., Inc., New York, N.Y., 1938).
[2] J. R. Pierce, Theory and design of electron beams, p. 43 (D. Van Nostrand Co., Inc., New York, N.Y., 1954).
[3] J. E. Rosenthal, Correction of deflection defocusing in CRT's, Proc. I.R.E. **39,** 10 (1951).
[4] R. G. E. Hutter, Electron beam deflection J. Appl. Phys. **18,** 797 (1947).
[5] R. G. E. Hutter, Advances in electronics, Vol. I, p. 167 (Academic Press, New York, N.Y., 1949).

WASHINGTON, D.C. (Paper 64C2–30)